Production of large-volume negative-ion source using multistring-type CF_4 magnetized plasma

M Abid Imtiaz, Shuichi Tsuruta and Tetsu Mieno*

Department of Physics, Faculty of Science, Shizuoka University, Ooya, Suruga-ku, Shizuoka-shi 422-8529, Japan

E-mail: piero@sannet.ne.jp

Abstract

A multistring-type CF_4 plasma has been produced by setting a multihole-type metal obstacle plate in a magnetized electron cyclotron resonance (ECR) plasma. Separative diffusion of negative ions (F^-) has been realized in the region downstream of the obstacle plate around the string-type plasma columns. Langmuir probes are used to estimate negative-ion density using the modified Bohm model. The experiment reveals that F^- density is of the order of $10^{15} \sim 6\times10^{15}$ m^{-3} around the multistring-type plasma. The column-type negative-ion source with a diameter of about 20 cm and a cross section of about 300 cm^2 is realized, which could be scaled up by introducing more string plasmas. The ratio of negative-ion density to electron density around the plasma column is in the range of 10 to 150.

KEYWORDS: multistring-type plasma, large-volume negative-ion source, Langmuir probe, magnetized plasma, carbon tetra fluoride, fluorine negative ion, fine silicon etching

* Author to whom correspondence should be addressed.

1. Introduction

Plasma-charging damage in the microscopic etching in the production of high-quality LSIs is a big problem. The accumulated charge in the etching holes would break the insulation layer [1] or cause side wall etching (notching) [2 – 4]. To minimize these problems plasma etching with negative ions has been tried [5, 6]. Large-area, high-density and stable negative-ion sources are expected to realize damagefree plasma etching in the production of higher-quality LSIs on a large silicon wafer [7]. By introducing negative-ion etching or etching using both positive and negative ions, the charge accumulation can be substantially reduced. Therefore, it is necessary to develop a high-density and large-diameter negative-ion source for noble negative-ion etching on a large silicon wafer.

A higher density of negative ions than electron density is reported to have been generated in low-density and low-electron-temperature plasmas of electronegative gases [8, 9]. It is now known that a magnetized plasma column generated from an electronegative gas tends to diffuse negative ions separately around the plasma column via radial diffusion [10]. Accumulation of high-density negative ions (F^-) using a hollow-type ECR CF_4 plasma has already been developed [11, 12]. For the production of negative ions, pulse-time-modulated discharges of electronegative gas [13, 14], low-power radio-frequency discharges of electronegative gas [9, 15], a magnetic filter in radio-frequency discharge [16] have also been developed. However, these negative-ion sources do not have a large plasma volume corresponding to the practical etching size.

To produce a large-area and high-density negative-ion source, we have focused on the construction of a special ion source with a multistring-type magnetized plasma. Here, “string” refers to a thin plasma column confined in a magnetic field. This plasma is realized by setting an obstacle plate with multiholes in an ECR plasma column.

A model for the expected mechanism of negative-ion confinement in the multistring-type plasma obtained by introducing CF_4 gas is illustrated in figure 1. The Larmor radius of electrons is much smaller than that of fluorine negative ions and, therefore, the perpendicular diffusion coefficient of negative ions is much higher than that of electrons. At the same time, reflection of F^- ions due to sheath potential at the boundaries would cause F^- ions to separate from electrons around each string-type plasma to make an ion-ion plasma. Clearly, increasing the number of strings of plasma arranged in an adjacent interval would result in a larger area for the production of negative ions, where selecting the diameter of the string-type plasmas and the distance among them is important for optimizing the volume of negative ions produced using the obstacle plate.

In this study, the large-volume F^- ion source has been produced by modifying the ECR CF_4 plasma. The hole diameter dependence of the obstacle plate, the reflection of F^- ions at the boundary, and the *x*-axis density profiles of F^- ions and electrons are investigated, and the optimum condition for F^- ion separation is studied. A large area for the production of negative ions is exhibited by the multistring-type plasma in the region downstream of the obstacle plate.

2. Brief theory

When a weak electronegative plasma is considered, where $n_-/n_e < 2$ (n_-: negative-ion density, n_e: electron density), the normal Bohm condition can be used at the sheath region of the plasma boundary, and n_- can be estimated from the Langmuir probe measurement [11]. The flow of positive ions to the probe is accelerated by the presheath potential $\Delta\emptyset_{ps} = \kappa T_{eb}/2e$ (κ: Boltzmann constant, T_{eb}: electron temperature of bulk plasma, e: electron charge) at the presheath region, and positive ion saturation current density to the probe is given by

$$J_{is} \approx \exp\left(-\frac{1}{2}\right) en_{ib}\sqrt{\frac{\kappa T_{eb}}{M_+}}, \tag{1}$$

where n_{ib} and M_+ stand for the positive-ion density in bulk plasma and the positive-ion mass, respectively [11, 17]. The subscript "b" denotes the bulk plasma.

On the other hand, in the presence of many negative ions $(n_-/n_e \geq 2)$, the presheath potential $\Delta\emptyset_{ps}$ is reduced, and this potential would reflect a quantity of the negative ions in the presheath region. In this article, this condition is called "the modified Bohm condition". In this condition, equation (1) should be modified [12, 18], and the ion saturation current density flowing to the probe is given by

$$J_{is} \approx e\left\{n_{eb}\exp\left(-\frac{e\Delta\emptyset_{ps}}{\kappa T_{eb}}\right) + n_{-b}\exp\left(-\frac{e\gamma\Delta\emptyset_{ps}}{\kappa T_{eb}}\right)\right\} \times \sqrt{\frac{2e\Delta\emptyset_{ps}}{M_+}}, \tag{2}$$

where n_{eb} and n_{-b} are the electron density and negative-ion density in bulk plasma, respectively, and $\gamma = T_{eb}/T_{-b}$ (ratio of electron temperature to negative-ion temperature in bulk plasma) [12].

According to the calculation method described in reference 11, we can evaluate n_{-b}/n_{eb} from the probe data, where the charge neutrality condition in the bulk plasma, $n_{eb} + n_{-b} = n_{ib}$ (n_{ib}: positive-ion density in bulk plasma) is used. Probe data at a reference point are used, where negative-ion density is negligible, and the charge neutrality, $n_{e0} = n_{i0}$ (n_{e0} and n_{i0}: electron density and positive-ion density at the reference point, respectively) is satisfied. Using equations (1) and (2),

$$\frac{n_{-b}}{n_{eb}} \approx \frac{J_{is}/n_{eb}}{J_{is0}/n_{e0}}\exp\left(\frac{e\gamma\Delta\emptyset_{ps}}{\kappa T_{eb}} - \frac{1}{2}\right)\sqrt{\frac{\kappa T_{e0}}{2e\Delta\emptyset_{ps}}} - \exp\left\{\frac{e\Delta\emptyset_{ps}(\gamma-1)}{\kappa T_{eb}}\right\}, \tag{3}$$

where J_{is0} and T_{e0} stand for the positive ion current density and electron temperature at the reference point, respectively. Presheath potential $e\Delta\emptyset_{ps}/\kappa T_{eb}$ as a function of n_{-b}/n_{eb} can be evaluated for different values of γ from the modified Bohm method, as stated in equations (6.4.9) and (6.4.10) in

reference 18. Therefore, n_{-b}/n_{eb} can be obtained by measuring $\frac{J_{is}/n_{eb}}{J_{is0}/n_{e0}}$, T_{eb} and T_{e0} and using equation (3) and figure 3 of reference 12, where the asymptotic method in the graph is utilized.

When $e\Delta\emptyset_{ps}$ is smaller than the positive-ion temperature in the bulk plasma, κT_{+b}, the ion saturation current to the probe is influenced by the thermal ion flow [12]. In this experiment, both κT_{+b} and negative-ion temperature κT_{-b} are assumed to be 0.1 eV, which is suitable for usual low-pressure laboratory plasmas [19, 20], and the effect of positive-ion temperature on the n_{-b}/n_{eb} evaluation can be neglected.

3. Experimental procedure

A schematic diagram of the experimental setup is shown in figure 2. A vacuum vessel made of stainless steel, 2.0 m in length and 21 cm in diameter, is set across 8 solenoid coils. In order to obtain a stable ECR region, the coils are positioned so as to produce a plateau region of the magnetic field of about 0.087 tesla at a distance 80 cm from the microwave window (z = 0 in the graph). An almost flat distribution of magnetic field of about 0.075±0.005 tesla has been maintained in the downstream region of the obstacle plate to produce the multistring-type plasma as shown in figure 2(a). A magnetron microwave generator ($f = 2.45$ GHz, $P_{\mu} = 0-1$ kW, Aikohdenki Co., ECR-04) is used to inject a continuous microwave through a quartz window into the plasma chamber. A metal end plate, 20 cm in diameter, which is electrically grounded, is placed at a location about 38 cm in the downstream region of the obstacle plate. Two hot-wire-type Langmuir probes are placed at locations 23 cm downstream and 8 cm upstream region of the obstacle plate. The electrode is made of Ta wire of 0.2 mm diameter, having the shape of a half-circle with an exposed tip area of 1.5 mm^2. J_{is0}/n_{e0} and T_{e0} are measured at a reference point in the upstream region of the obstacle plate (26 cm toward the obstacle plate from the ECR point and center of the x-axis), where the negative-ion density is negligible [11].

At about 34 cm downstream of the ECR point, a special obstacle plate with 12 small holes of diameter d_h = 2.0 cm is placed under electrically grounded conditions as shown in figure 2(b). The holes have a two-dimensional lattice structure with lattice distance a_0 = 6.0 cm. Plasma flows into the region downstream of the obstacle plate through these holes, thereby producing a bundle of string-type plasmas. The holes in the obstacle plate are positioned in such a way that the rows of the strings of plasma are horizontal, and the probes are moved on the x-axis in figure 2(b), where the probe at the downstream position does not cross the string-type plasma region. To determine the optimum diameter and the positions of the holes in the obstacle plate, an experiment is performed using a single-columned plasma, which is produced using an obstacle plate with a single hole at the center. The hole diameters d_h = 1.0, 2.0, 3.0 and 5.0 cm are examined. The x-axis distributions of n_- in the downstream region (23 cm towards the end plate from the single-hole obstacle plate) obtained for each hole size are shown in figure 3, where $p(CF_4)$ = 0.13 Pa and P_{μ} = 170 W, and the modified Bohm

method is used. Δr is the radial distance from the hole rim. It is evident that the maximum values of negative-ion density for the three larger holes are almost the same. However, the larger holes reduce the volume of the negative-ion region. On the basis of these data, a multihole-type obstacle plate is designed, as shown in figure 2(b), where $a_0 = 6.0$ cm. The geometrical efficiency of negative-ion accumulation, η, which is defined by S_- / S_{total} (S_-: cross section of negative-ion region, S_{total}: cross section of bulk ECR plasma), the average density of negative ions in the negative-ion region, n_{av}, which is estimated from the results of figure 3, where the axial symmetry of n_- is assumed, and the total number of negative ions, N_{total}, which is the number of F^- ions in the triangle pole with unit height as is in figure 2(b), are calculated and shown in table 1. From the table, the geometrical efficiencies of the large-hole types are very small compared to those of smaller-hole types. However, with the aim of obtaining the best possible results, optimizing the values of η, N_{total} and lattice distance a_0 is under investigation. In this study, $d_h = 2.0$ cm and $a_0 = 6.0$ cm are adopted.

4. Results and discussion

Figure 4(a) shows typical x-axis profile of n_- measured by the probe, and evaluated by the modified Bohm model and the normal Bohm model at a typical microwave input power of $P_\mu = 170$ W and a CF_4 gas pressure of $p = 0.19$ Pa. The calculation of n_- under the normal Bohm condition [12], which is not exact, is about 10 times lower than that under the modified Bohm condition. In order to check the effect of superposition of diffused negative ions from the plasma columns, the distribution of n_- along the x-direction (along which measurements are carried out by the probe) is artificially made by using the data from one string plasma as shown in figure 3. In this case, superposition of negative ions from each string plasma is assumed to generate n_- distribution. From figure 4(b), it is evident that a simple superposition of strings would result in a flat and large-area production of negative ions supporting the measurement of figure 4(a).

Figure 5(a) shows typical x-axis distributions of electron density n_e at the two measurement positions ($x \geq 0$), at a typical microwave input power of $P_\mu = 300$ W and a CF_4 gas pressure of $p =$ 0.12 Pa, where $x = 0$ refers to the axial center. The electron density at the upstream position (26 cm toward the obstacle plate from the ECR) is about 20 times higher than that at the downstream position (23 cm towards the end plate from the multihole obstacle plate) around the multistring-type plasma region, and flat x-axis distributions of n_e are observed at both the upstream and downstream positions. The x-axis distribution of negative-ion density n_- evaluated using the modified Bohm is shown in figure 5(b), where n_- is. It is hypothesized that activated CF_4 molecules effectively produce F^- ions at the rim region of the string-type plasma [21]. The x-axis profiles of plasma potential $\emptyset_p$ and floating potential $\emptyset_f$ at the downstream position are shown in figure 5(c). There are some effects caused by the positions of the plasma columns. It can be confirmed that the plasma potential around

the string-type plasmas which is everywhere positive corresponds to the end-plate potential (grounded potential). Therefore, almost all negative ions are reflected at the axial ends and confined well. In this study, positive ions would not be confined well and they flow towards the boundaries. The *x*-axis profile of T_e at the downstream position is shown in figure 5(d). T_e varies from 1.2 to 2.8 eV throughout the *x*-direction ($x \geq 0$) around the multistring-type plasma.

The *x*-axis profiles of negative-ion density and n_-/n_e at the downstream of the obstacle plate for several pressures (at P_μ= 300 W) are measured and shown in figure 6, where the modified Bohm method is used. By increasing the pressure from p = 0.078 Pa to 0.12 Pa, both n_-, n_e and n_-/n_e gradually decrease. It is conjectured that the higher collision frequency among electrons and CF_4 molecules would reduce the production rate of excited molecules to make F^- ion via dissociation.

The *x*-axis profiles of negative-ion density and n_-/n_e at the downstream of the obstacle plate for several powers (at p= 0.12 Pa) are measured and shown in figures 7(a) and 7(b), where the modified Bohm method is used. By increasing the input power from P_μ= 170 W to 300 W, both n_- and n_-/n_e decrease, even though n_e gradually increases. T_e at x = 3 cm vs P_μ is also shown in figure 7(c). It is speculated that the higher input energy increases the electron temperature, and the high-energy electrons would reduce the production rate of negative ions or neutralize F^- ion at the boundary of the multistring-type plasma.

5. Conclusions

The volume of negative ions produced in a single-column plasma is limited by simple radial diffusion. In order to obtain a large-volume negative-ion source, a multistring-type plasma has been developed. In this study, an obstacle plate is set in ECR plasma to produce adequate multistring-type plasma. For the effective negative-ion source multiholes with d_h = 2.0 cm and a_0 = 6.0 cm in the obstacle plate are adopted, resulting in production of a large-volume and stable source of negative ions (F^-). The diameter of the ion source is about 20 cm and its cross section is about 300 cm^2. The geometrical efficiency is about 90%. n_- around the string-type plasmas is of the order of 10^{15} to 6×10^{15} m^{-3}, and n_-/n_e ranges from about 10 to 150. The obstacle plate design, CF_4 gas pressure, microwave power and magnetic field are the variable parameters used to control the volume and density of negative ions, which would make large-diameter negative-ion source and are under investigation. A flatter n_- profile and higher-efficiency production of F^- ions are also under investigation.

Acknowledgement

This work is supported by a grant-in-aid from the Ministry of Education, Culture, Sports, Science and Technology (MEXT), Japan.

References

[1] Cheung K P and Chang C P 1994 *J. Appl. Phys.* **75** 4415.

[2] Ootera H, Oomori T, Tuda M and Namba K 1994 *Jpn, J, Appl. Phys.* **33** 4276.

[3] Nozawa T, Kinoshita T, Nishizuka T, Narai A, Inoue T and Nakaue A 1995 *Jpn, J, Appl. Phys.* **34** 2107.

[4] Kinoshita T, Hane M and McVittie J P 1996 *J. Vac. Sci. & Technol.* **B 14** 560.

[5] Shindo H, Sawa Y and Horiike Y 1995 *Jpn. J. Appl. Phys.* **34** L925.

[6] Shibayama T, Shindo H and Horiike Y 1996 *Plasma Sources Sci. Technol.* **5** 254.

[7] Samukawa S, Ohtake H and Mieno T 1996 *J. Vacuum Sci. & Technol.* **A 14** 3049.

[8] Shindo M, Uchino S, Ichiki R, Yoshimura S and Kawai Y 2001 *Rev. Sci. Instrum.* **72** 2288.

[9] Haverlag M, Kono A, Passchier D, Kroesen G M W, Goedheer W J and deHoog F J 1991 *J. Appl. Phys.* **70** 3472.

[10] Sato N 1994 *Plasma Sources Sci. Technol.* **3** 395.

[11] Kawai R, Mieno T 1997 *Jpn. J. Appl. Phys.* **36** L1123.

[12] Mieno T, Ogawa A 1999 *Jpn. J. Appl. Phys.* **38** 4586.

[13] Mieno T, Kamo T, Hayashi D, Shoji T and Kadota K 1996 *Appl. Phys. Lett.* **69** 617.

[14] Mieno T and Samukawa S 1995 *Jpn. J. Appl. Phys.* **34** L1079.

[15] Kono A, Haverlag M, Passchier D, Kroesen G M W, and deHoog F J 1991 *J. Appl. Phys.* **70** 2939.

[16] Amemiya H 1991 *Jpn. J. Appl. Phys.* **30** 2601.

[17] Hershkowitz N 1989 *Plasma diagnostics* vol 1, ed O Auciello and D L Flamm (San Diego: Academic Press Inc.) p 125.

[18] Lieberman M A and Lichtenberg A J 1994 *Principles of Plasma Discharges and Materials Processing* (New York: Wiley) p 167.

[19] Nakano T, Ohtake H and Samukawa S 1996 Abstract *189th Meet. Electrochemical Society, Los Angeles* vol 96-1 (Pennington, NJ: The Electrochemical Society) p 228.

[20] Woo H -J, Chung K -S, Lho T 2006 Proceedings *6th Int. Conf. Reactive Plasmas, Sendai* (Tokyo: Jpn. Soc. Applied Physics) p 779.

[21] Stoffels E, Stoffels W W and Kroesen G M W 2001 *Plasma Sources Sci. Technol.* **10** 311.

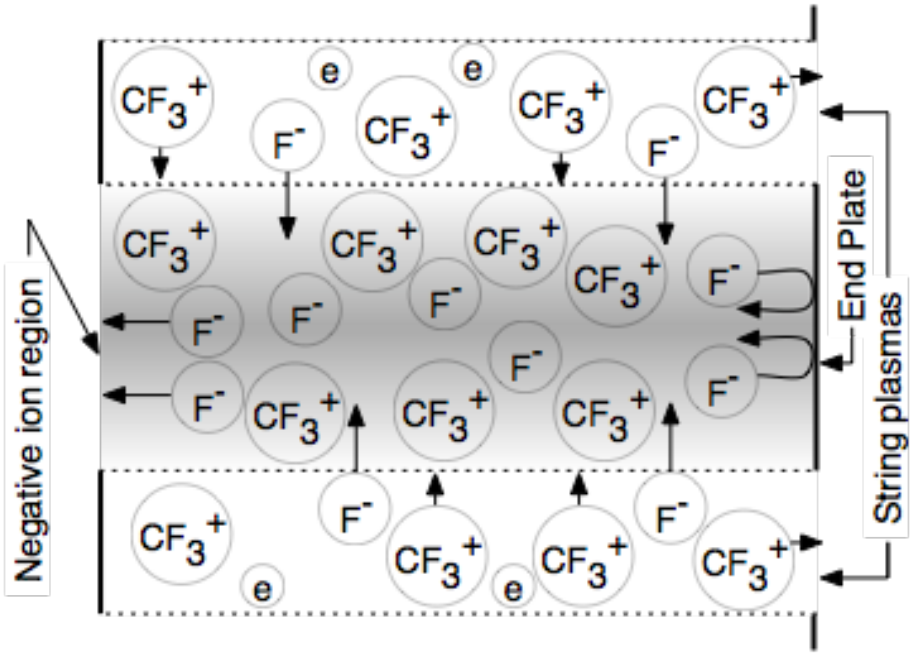

Figure 1. Model figure of accumulation of negative ions between adjacent string plasma columns via diffusion and reflection of F^- ions at boundaries.

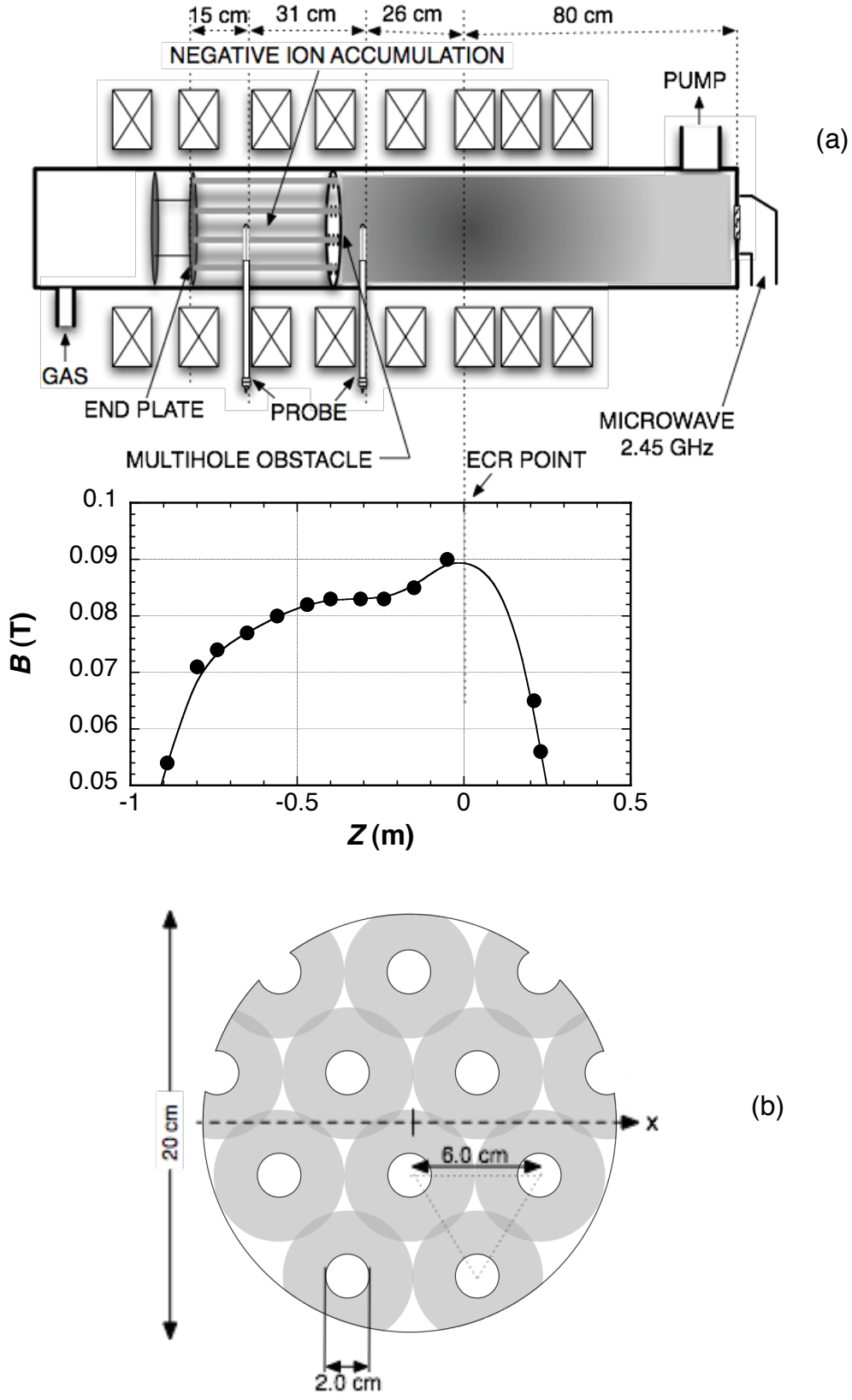

Figure 2. Schematic of experimental setup and axial distribution of magnetic field (a). Multihole-type metal obstacle plate (b).

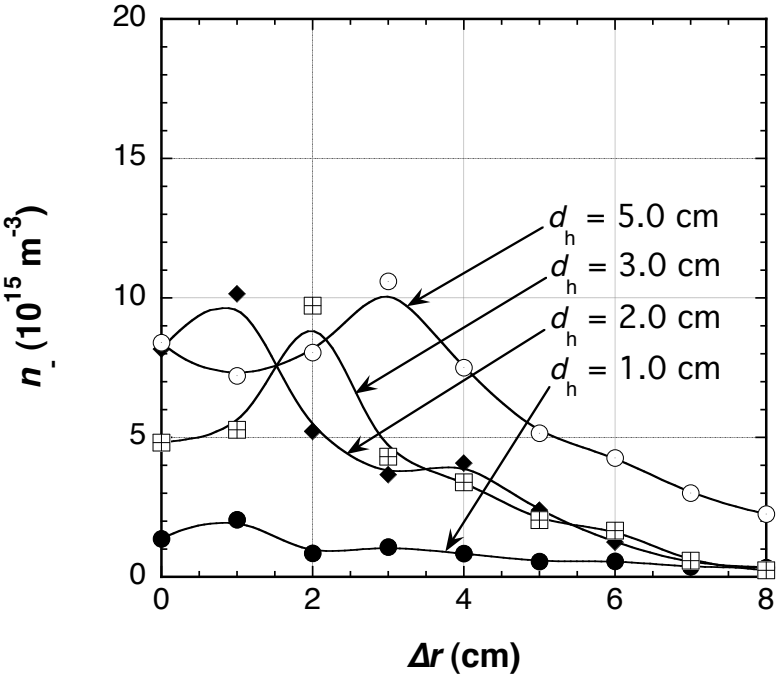

Figure 3. Radial profiles of n_- for four hole diameters, where only one hole is made on an obstacle plate at radial center. Δr is horizontal position measured from the rim of the hole. P_μ = 170 W and p = 0.13 Pa.

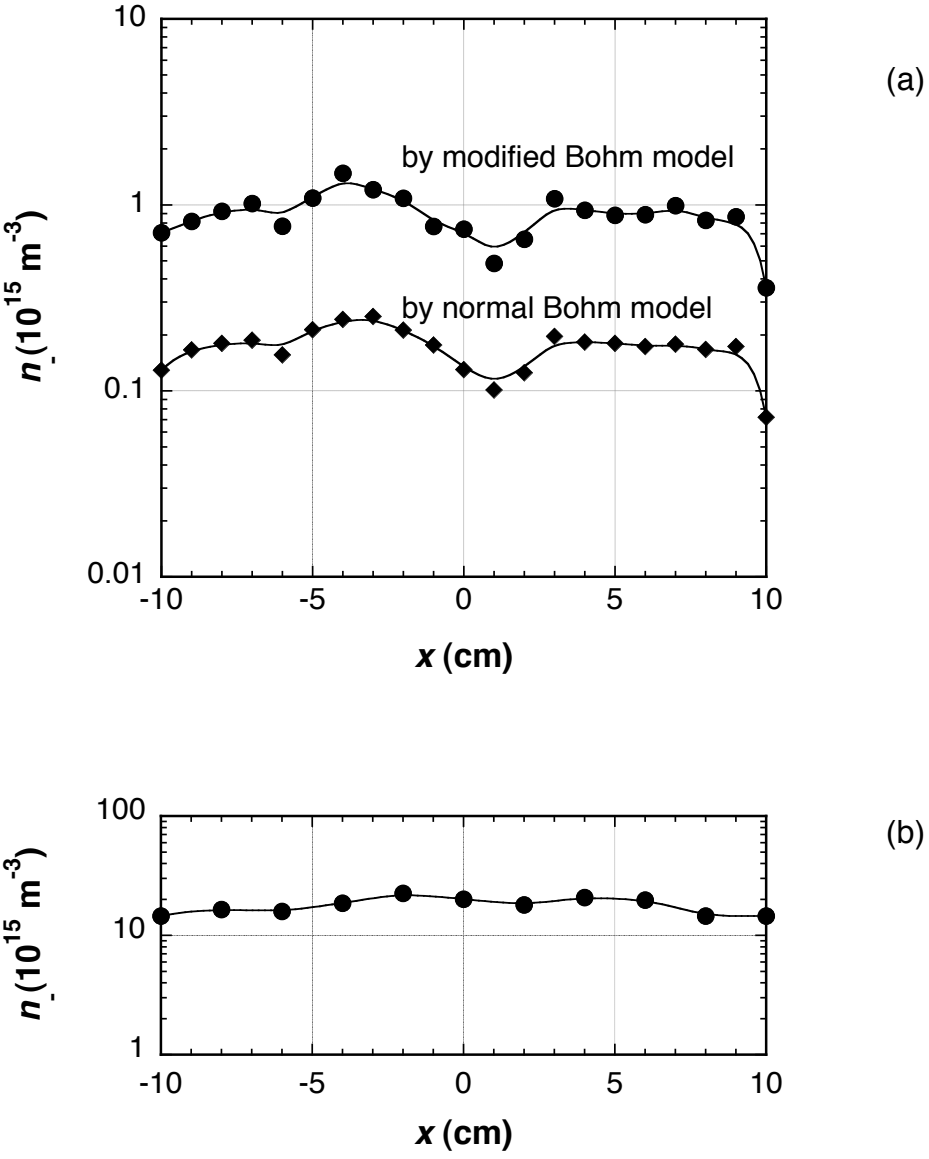

Figure 4. x-axis profiles of n_- measured by a probe and evaluated by two methods over 20 cm diameter (a). P_μ = 170 W and p = 0.19 Pa. x-axis distribution of n_- as in figure (b), which is calculated by simple superposition of n_- produced by one plasma column (d_h = 2.0 cm) shown in figure 3.

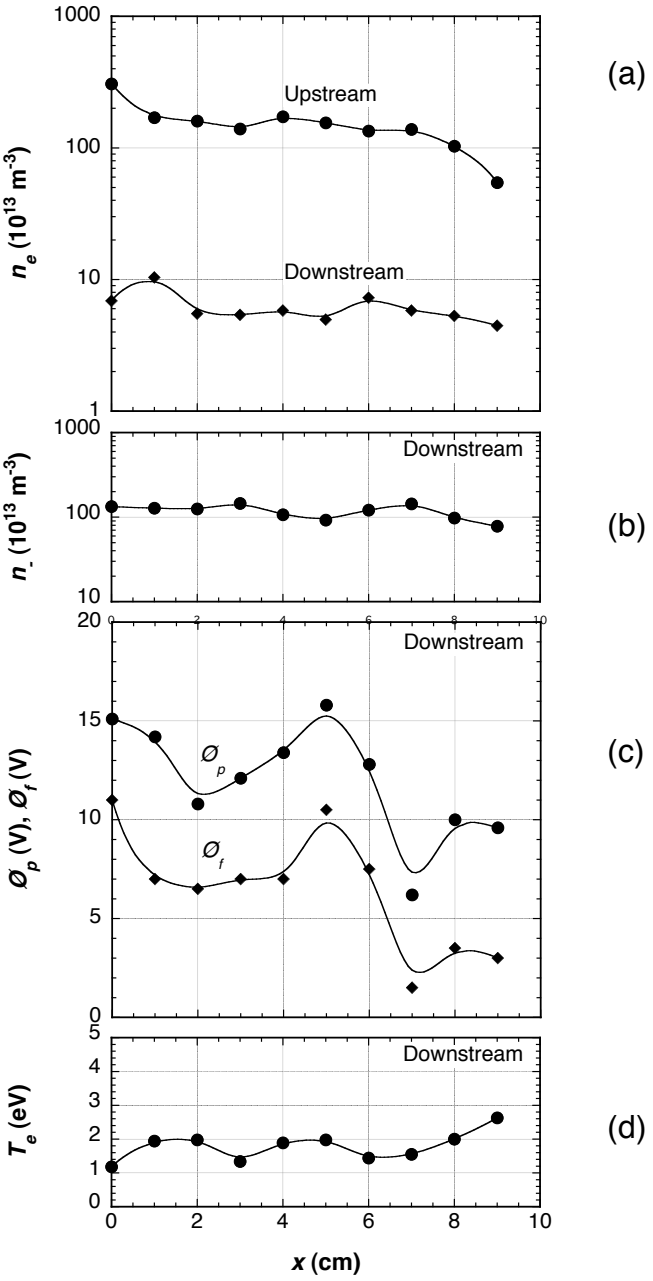

Figure 5. Typical x-axis distributions of n_e at two positions (a), n_- at downstream position (b), plasma potential $Ø_p$ and floating potential $Ø_f$ at downstream position (c), and T_e at downstream position (d). P_μ = 300 W and p = 0.12 Pa.

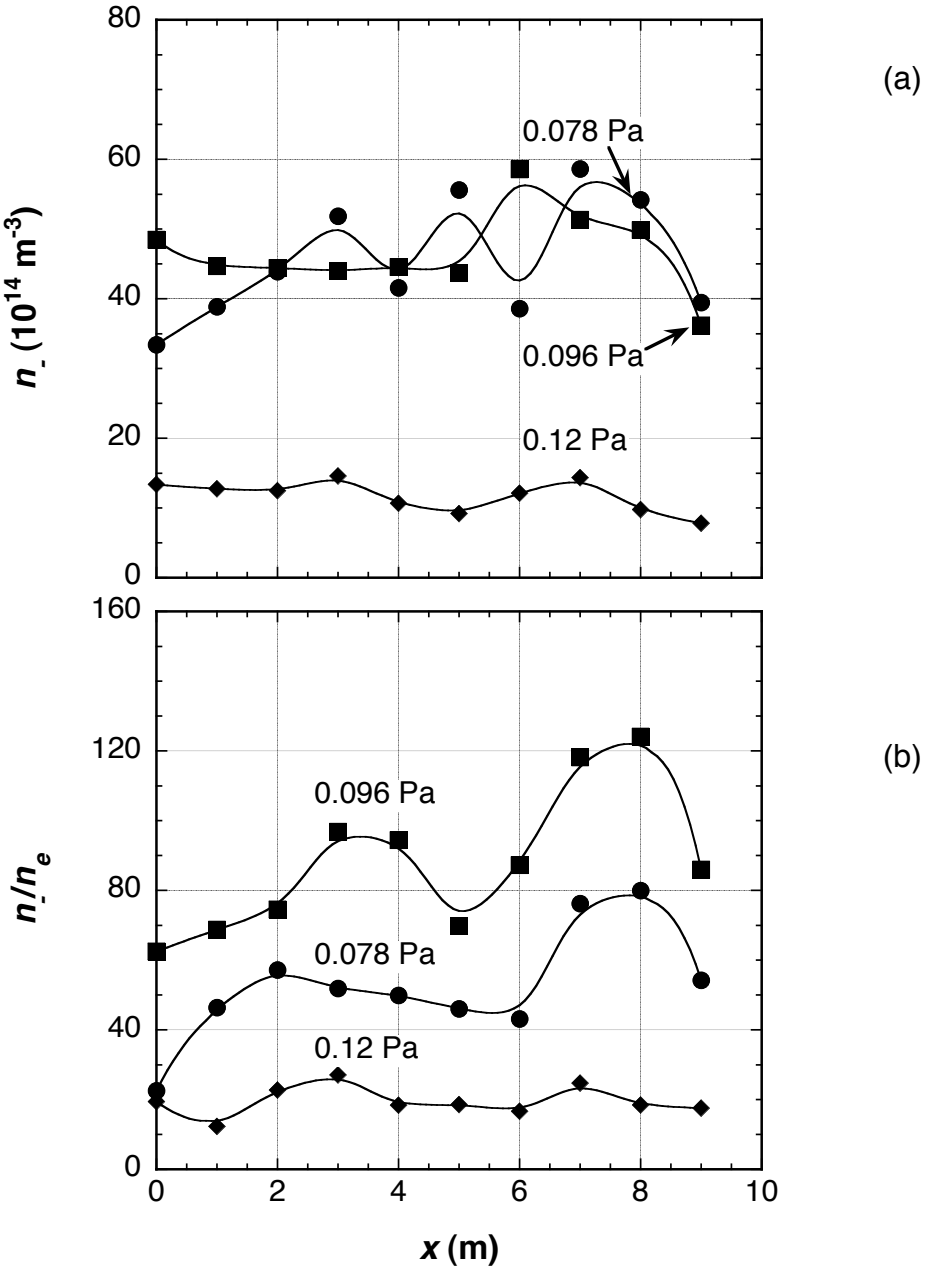

Figure 6. x-axis distributions of n_- (a) and n_-/n_e (b) at downstream position for three pressures. P_μ = 300 W.

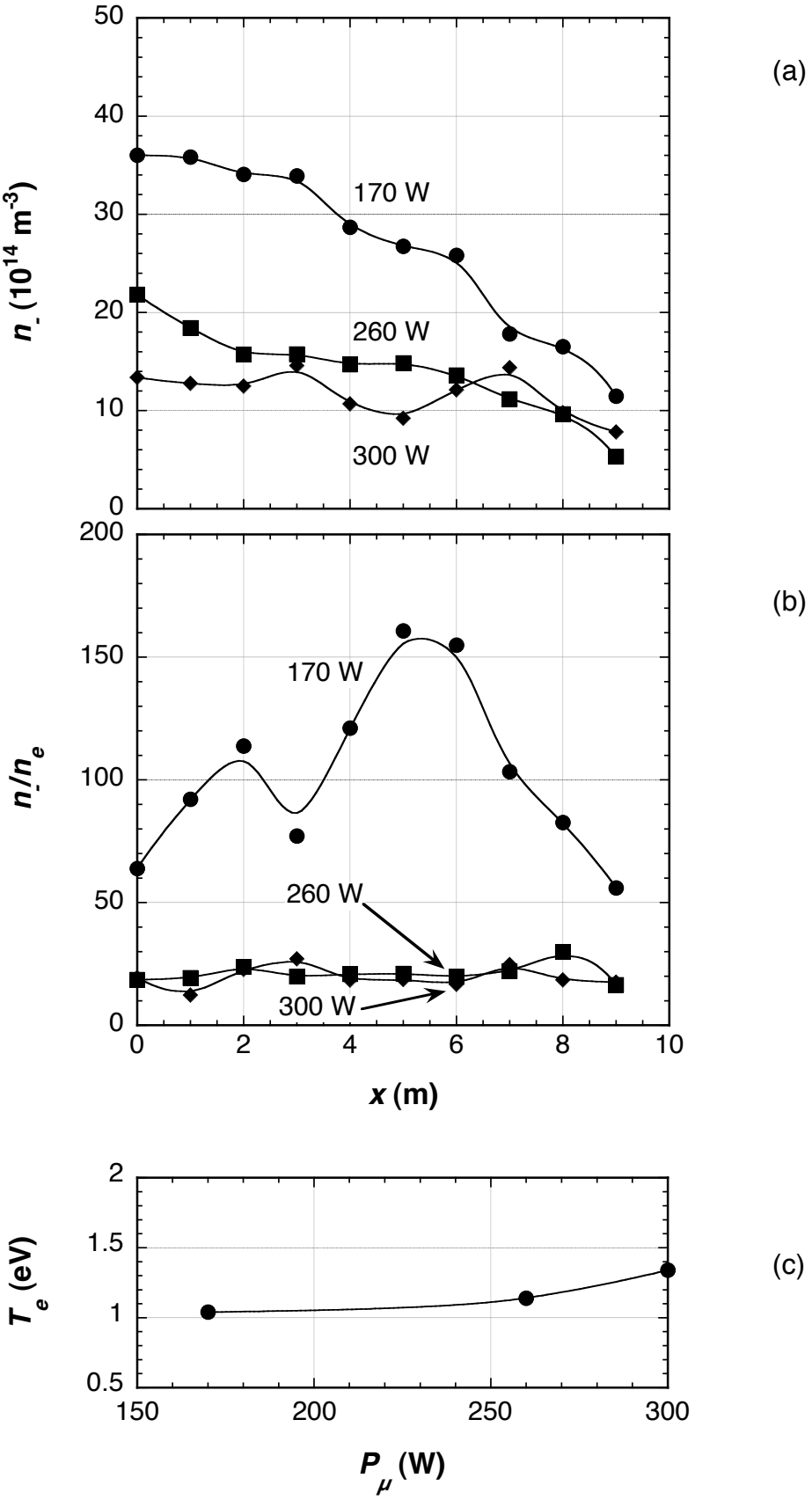

Figure 7. x-axis distributions of n_- (a) and n_-/n_e (b) at downstream position for three input powers. T_e vs P_μ at x = 3 cm (c). p = 0.12 Pa.

Table 1. The geometrical efficiency of negative ion accumulation, η, the average density of negative ions in the negative ion region, n_{av}, and the total number of negative ions in the triangle pole with unit height as is in figure 2(b), N_{total}. d_h is a hole diameter.

d_h (cm)	$\eta(\%) = S_- / S_{total}$	n_{av} (m^{-3})	N_{total} (m^{-1})
1.0	97.44	3.16×10^{15}	4.80×10^{12}
2.0	89.74	1.24×10^{16}	1.74×10^{13}
3.0	77.56	1.41×10^{16}	1.71×10^{13}
5.0	37.05	1.11×10^{15}	6.42×10^{11}